

CONVERGENCE OF ADAPTIVE MIXED FINITE ELEMENT METHOD FOR CONVECTION-DIFFUSION-REACTION EQUATIONS*

SHAOHONG DU[†] AND XIAOPING XIE[‡]

Abstract. We prove the convergence of an adaptive mixed finite element method (AMFEM) for (nonsymmetric) convection-diffusion-reaction equations. The convergence result holds from the cases where convection or reaction is not present to convection-or reaction-dominated problems. A novel technique of analysis is developed without any quasi orthogonality for stress and displacement variables, and without marking the oscillation dependent on discrete solutions and data. We show that AMFEM is a contraction of the error of the stress and displacement variables plus some quantity. Numerical experiments confirm the theoretical results.

Key words. adaptive mixed finite element method, quasi orthogonality, oscillation, convergence

AMS subject classifications. 65N30, 65N15, 65N12, 65N50

1. Introduction and main results. Let Ω be a bounded polygonal or polyhedral domain in \mathbb{R}^d , $d = 2$ or 3 . We consider the following convection-diffusion-reaction equations:

$$\begin{cases} -\nabla \cdot (S\nabla p) + \nabla \cdot (p\mathbf{w}) + rp = f & \text{in } \Omega, \\ p = 0 & \text{on } \partial\Omega, \end{cases} \quad (1.1)$$

where $S \in L^\infty(\Omega; \mathbb{R}^{d \times d})$ is an inhomogeneous and anisotropic diffusion-dispersion tensor, \mathbf{w} is a (dominating) velocity field, r is a reaction function, and f is a source term. The choice of homogeneous boundary conditions is made for ease of presentation, since similar results are valid for other boundary conditions.

Adaptive methods for the numerical solution of PDEs are now standard tools in science and engineering to achieve better accuracy with minimum degrees of freedom. The adaptive procedure of (1.1) consists of loops of the form

$$\text{SOLVE} \rightarrow \text{ESTIMATE} \rightarrow \text{MARK} \rightarrow \text{REFINE}. \quad (1.2)$$

A posteriori error estimation (ESTIMATE) is an essential ingredient of adaptivity, and reaches its mature level after two decades of development [1, 3, 4, 5, 11, 12, 18, 38]. However, the analysis of convergence of the whole algorithm (1.2) is still in its infancy, and is carried out mainly for standard adaptive finite element methods (AFEM) [8, 23, 30, 31, 32].

Due to the saddle-point characteristic of mixed finite element approximation, there is no orthogonality available, as is one of main difficulties in the convergence analysis of AMFEM. Thus one has to find some quasi-orthogonality instead of the orthogonality, and the occurrence of oscillation of data is inevitable. Hence, how to deal with the oscillation becomes a key issue in the analysis. For the convergence of AMFEM, the present studies mainly focus on Poisson equations. In [10], *Carstensen* and *Hoppe* proved the error reduction and convergence for the lowest-order Raviart-Thomas element with marking the data oscillation. *Chen*, *Holst* and *Xu* [14] showed the convergence of a quasi-error with marking the data oscillation.

*This work was supported in part by The Natural Science Foundation of Chongqing city under Grant No. CSTC, 2010BB8270, The Education Science Foundation of Chongqing (KJ120420), The National Natural Science Foundation of China (11171239), The Project-sponsored by Scientific Research Foundation for the Returned Overseas Chinese Scholars and Open Fund of Key Laboratory of Mountain Hazards and Earth Surface Processes, CAS.

[†]School of Science, Chongqing Jiaotong University, Chongqing 400047, China. (*dushhong@gmail.com*).

[‡]Corresponding author. School of Mathematics, Sichuan University, Chengdu 610064, China (*xpx-iec@gmail.com*).

In [6, 13, 19], the convergence was analyzed for the lowest-order Raviart-Thomas element where the local refinement was performed by using only either the estimators or the data oscillation term.

For general diffusion problems and more general mixed elements, by using the orthogonality of the divergence of the flux, *Du* and *Xie* [20] showed the convergence of the flux error plus some quantity without marking the oscillation.

The purpose of this paper is to prove the following convergence results for an AMFEM for the convection-diffusion-reaction equations (1.1) and verify them computationally.

THEOREM 1.1. (Convergence of AMFEM) *Denote by $\{\mathcal{T}_k, e_k^2, A_k^2\}_{k \geq 0}$ the sequence of meshes, the error of the stress and displacement variables, and some quantity (defined by (5.12)) produced by the AMFEM algorithm. Let h_0 be the mesh size of the quasi-uniform initial mesh \mathcal{T}_0 . Then there exist two positive constants q and $\alpha \in (0, 1)$ such that*

$$e_{k+1}^2 + (1 - h_0 q) A_{k+1}^2 \leq \alpha^2 (e_k^2 + (1 - h_0 q) A_k^2)$$

when $h_0 \leq \frac{1 - \alpha^2}{1 + \alpha^2} \frac{1}{q}$. This means that AMFEM, as h_0 is small enough, converges with a linear rate α , namely,

$$e_k^2 + (1 - h_0 q) A_k^2 \leq \alpha^{2k} (e_0^2 + (1 - h_0 q) A_0^2).$$

This theorem extends the convergence results in [20] in the following several aspects.

- We deal with more general convection-diffusion-reaction equations here with variable coefficients S , \mathbf{w} and r , whereas in [20] \mathbf{w} and r vanish.
- The orthogonality for the divergence of the flux is absent due to the convection term $\mathbf{w} \cdot \nabla p$ and the zero order term $(r + \nabla \cdot \mathbf{w})p$. So this contribution considers not only the flux (stress variable) error but also the displacement variable error.
- The quasi-orthogonality for stress and displacement variables also fails due to the terms $\mathbf{w} \cdot \nabla p$ and $(r + \nabla \cdot \mathbf{w})p$. This will lead to an additional constraint on the mesh size, h_0 , of the quasi-uniform initial mesh \mathcal{T}_0 .
- The oscillation term depends on the discrete solution and data. Therefore, the oscillation and error can not be reduced separately here. In [20] the oscillation term is not included in the a posteriori indicators.
- Since the error and oscillation are now coupled, in order to prove convergence without marking the oscillation term, we need to handle them together by following the same idea as in [16, 26].
- In comparison with previous analysis methods, we consider the a posteriori indicators with weighted factors. We also release the constraint that the divergence of the convection term is free in contrast to the analysis of standard AFEM (see [27]).

The rest of this paper is organized as follows. Section 2 gives some preliminaries and details on notations. Section 3 derives an estimate for the error between L^2 -projection of the displacement and its approximation solution, which is key to the convergence analysis. Section 4 shows the estimator reduction. We prove theorem 1.1 (Convergence of AMFEM algorithm) in section 5 and present four numerical experiments to illustrate properties of AFMEM in section 6.

2. Assumptions, weak problem, and AMFEM algorithm. For a domain $A \subset \mathbb{R}^d$, we denote by $L^2(A)$ and $\mathbf{L}^2(A) := (L^2(A))^d$ the spaces of square-integrable functions, by $(\cdot, \cdot)_A$ the $L^2(A)$ or $\mathbf{L}^2(A)$ inner product, by $\|\cdot\|_A$ the associated norm, and by $|A|$ the Lebesgue measure of A . Let $H^k(A)$ be the usual Sobolev space equipped with norm $\|\cdot\|_{k,A}$ for $k = 1, 2$; $H_0^1(A) := \{v \in H^1(A) : v|_{\partial A} = 0\}$, $H(\text{div}, A) := \{\mathbf{v} \in \mathbf{L}^2(A) : \text{div } \mathbf{v} \in$

$L^2(A)$. $\langle \cdot, \cdot \rangle_{\partial A}$ denotes $d - 1$ -dimensional inner product on ∂A for the duality pairing between $H^{-1/2}(\partial A)$ and $H^{1/2}(\partial A)$. In what follows we shall omit the subscript Ω when $A = \Omega$.

Let \mathcal{T}_h be a shape regular triangulation in the sense of [15], and denote the mesh size $h_T := |T|^{1/d}$ with $|T|$ the area of $T \in \mathcal{T}_h$. Let C_Q be a positive constant depending only on a quantity Q , and $C_i (i = 1, 2, \dots)$ positive constants determined only by the shape regularity of \mathcal{T}_h . We denote by ε_h the set of element sides in \mathcal{T}_h , by ε_h^0 the set of interior sides of elements. For $K \in \mathcal{T}_h$, denote by ε_K the set of sides of K . Furthermore, we denote by ω_K and ω_σ the unions of all elements in \mathcal{T}_h respectively sharing a side with K and sharing a side $\sigma \in \varepsilon_h$. We use the "broken Sobolev space" $H^1(\cup \mathcal{T}_h) := \{\varphi \in L^2(\Omega) : \varphi|_K \in H^1(K), \forall K \in \mathcal{T}_h\}$. $H^2(\cup \mathcal{T}_h)$ is defined analogously. Denote by $[v]_\sigma := (v|_K)|_\sigma - (v|_L)|_\sigma$ the jump of $v \in H^1(\cup \mathcal{T}_h)$ over an interior side $\sigma := K \cap L$ of diameter $h_\sigma := \text{diam}(\sigma)$, shared by the two neighboring (closed) elements $K, L \in \mathcal{T}_h$. Especially, $[v]_\sigma := (v|_K)|_\sigma$ if $\sigma \subset \partial K \cap \partial \Omega$. Note that $[\cdot]$ is a linear operator over the broken Sobolev space $H^1(\cup \mathcal{T}_h)$.

We note that throughout the paper, the local version of differential operator ∇ is understood in the distribution sense, namely, $\nabla_h : H^1(\cup \mathcal{T}_h) \rightarrow (L^2(\Omega))^d$ is defined with $\nabla_h v|_K := \nabla(v|_K)$ for all $K \in \mathcal{T}_h$.

Given a unit normal vector $\mathbf{n}_\sigma = (n_1, \dots, n_d)^T$ along the side σ with $d = 2, 3$, we define the tangential component of a vector $\mathbf{v} \in \mathbb{R}^d$ with respect to \mathbf{n}_σ by

$$\gamma_{\mathbf{t}_\sigma}(\mathbf{v}) := \begin{cases} \mathbf{v} \cdot (-n_2, n_1)^T & \text{if } d = 2, \\ \mathbf{v} \times \mathbf{n}_\sigma & \text{if } d = 3, \end{cases}$$

where \times denotes the usual vector product of two vectors in \mathbb{R}^3 .

Following [39], we suppose that there exists an original triangulation \mathcal{T}_0 of Ω such that data of the problem (1.1) are given in the following way.

Assumptions of data :

(D1) $S_K := S|_K$ is a constant, symmetric, and uniformly positive definite tensor such that $c_{S,K} \mathbf{v} \cdot \mathbf{v} \leq S_K \mathbf{v} \cdot \mathbf{v} \leq C_{S,K} \mathbf{v} \cdot \mathbf{v}$ holds for all $\mathbf{v} \in \mathbb{R}^d$ and all $K \in \mathcal{T}_0$ with $c_{S,K} > 0, C_{S,K} > 0$;

(D2) $\mathbf{w} \in RT_0(\mathcal{T}_0)$ (see below) and $|\mathbf{w}|_K| \leq C_{\mathbf{w},K}$ for all $K \in \mathcal{T}_0$ with $C_{\mathbf{w},K} \geq 0$;

(D3) $r_K := r|_K$ is a constant for all $K \in \mathcal{T}_0$;

(D4) $c_{\mathbf{w},r,K} := 1/2 \nabla \cdot \mathbf{w}|_K + r|_K \geq 0$ and $C_{\mathbf{w},r,K} := |\nabla \cdot \mathbf{w}|_K + r|_K|$ for all $K \in \mathcal{T}_0$;

(D5) $f \in L^2(\Omega)$;

(D6) if $c_{\mathbf{w},r,K} = 0$, then $C_{\mathbf{w},r,K} = 0$.

Note that in [21, 22] $f|_K$ is assumed to be a polynomial of degree at most k for each $K \in \mathcal{T}_0$ so as to derive the efficiency of the residual indicators. Here we relax the restriction of f (cf. (D5)).

Introduce the stress variable $\mathbf{u} := -S \nabla p$, the mixed variational problem of (1.1) reads as: Find $(\mathbf{u}, p) \in H(\text{div}, \Omega) \times L^2(\Omega)$ such that

$$(S^{-1} \mathbf{u}, \mathbf{v}) - (p, \nabla \cdot \mathbf{v}) = 0 \quad \text{for all } \mathbf{v} \in H(\text{div}, \Omega), \quad (2.1)$$

$$(\nabla \cdot \mathbf{u}, \varphi) - (S^{-1} \mathbf{u} \cdot \mathbf{w}, \varphi) + ((r + \nabla \cdot \mathbf{w})p, \varphi) = (f, \varphi) \quad \text{for all } \varphi \in L^2(\Omega). \quad (2.2)$$

Let $P_0(K)$ denote the set of constant functions on each $K \in \mathcal{T}_h$. We respectively define the lowest order Raviart-Thomas finite element ([35]) space and the piecewise constant space as following:

$$RT_0(\mathcal{T}_h) := \left\{ \mathbf{q}_h \in \mathbf{H}(\text{div}, \Omega) : \forall K \in \mathcal{T}_h, \exists \mathbf{a} \in \mathbb{R}^d, \exists b \in \mathbb{R}, \right. \\ \left. \text{such that } \mathbf{q}_h(\mathbf{x}) = \mathbf{a} + b\mathbf{x}, \text{ for all } \mathbf{x} \in K. \right\}$$

and

$$P_0(\mathcal{T}_h) := \{v_h \in L^\infty(\Omega) : \forall K \in \mathcal{T}_h, v_h|_K \in P_0(K)\}.$$

We note that $\nabla \cdot (RT_0(\mathcal{T}_h)) \subset P_0(\mathcal{T}_h)$.

The centered mixed finite element scheme (cf. [17, 39]) of (1.1) reads as: Find $(\mathbf{u}_h, p_h) \in RT_0(\mathcal{T}_h) \times P_0(\mathcal{T}_h)$ such that

$$(S^{-1}\mathbf{u}_h, \mathbf{v}_h) - (p_h, \nabla \cdot \mathbf{v}_h) = 0 \quad \text{for all } \mathbf{v}_h \in RT_0(\mathcal{T}_h), \quad (2.3)$$

$$(\nabla \cdot \mathbf{u}_h, \varphi_h) - (S^{-1}\mathbf{u}_h \cdot \mathbf{w}, \varphi_h) + ((r + \nabla \cdot \mathbf{w})p_h, \varphi_h) = (f, \varphi_h) \quad \text{for all } \varphi_h \in P_0(\mathcal{T}_h). \quad (2.4)$$

In what follows, we shall show an AMFEM algorithm based on the a posteriori error estimator developed in [21]. We note that our convergence analysis below is also valid for AMFEM based on the estimator proposed in [22].

Suppose that the module SOLVE outputs a pair of discrete solutions over \mathcal{T}_h , namely, $(\mathbf{u}_h, p_h) = \text{SOLVE}(\mathcal{T}_h)$. The estimator in [21] consists of several indicators with different weight factors, where the elementwise estimator $\eta_{\mathcal{T}_h}^2(\mathbf{u}_h, p_h, K)$ can, for convenience, be abbreviated to

$$\eta_{\mathcal{T}_h}^2(\mathbf{u}_h, p_h, K) := D_K^2 h_K^2 \|\mathbf{S}^{-1}\mathbf{u}_h\|_K^2 + \alpha_K^2 h_K^2 \|R_K\|_K^2 + \sum_{\sigma \in \varepsilon_K} D_\sigma^2 h_\sigma \|\llbracket \gamma_{\mathbf{t}_\sigma}(\mathbf{S}^{-1}\mathbf{u}_h) \rrbracket\|_\sigma^2.$$

Here $\alpha_K = \min(h_K/\sqrt{c_{S,K}}, 1/\sqrt{c_{\mathbf{w},r,K}})$, R_K is the elementwise residual defined by

$$R_K := f - \nabla \cdot \mathbf{u}_h + (\mathbf{S}^{-1}\mathbf{u}_h) \cdot \mathbf{w} - (r + \nabla \cdot \mathbf{w})p_h,$$

and D_K, D_σ denote two variants of coefficients over each element $K \in \mathcal{T}_h$ and each side $\sigma \in \varepsilon_h$ respectively given by

$$D_K^2 := c_{\mathbf{w},r,K} + C_{\mathbf{w},r,K}^2 \alpha_K^2 + \max_{K': K' \cap K \neq \emptyset} c_{\mathbf{w},r,K'} + \max_{K': K' \cap K \neq \emptyset} \frac{|\nabla \cdot \mathbf{w}|_{K'}}{c_{\mathbf{w},r,K'}},$$

$$D_\sigma^2 := \frac{1}{2} \max_{K: \bar{K} \cap \bar{\sigma} \neq \emptyset} C_{S,K} + \frac{1}{2} \min\left\{ \max_{K: \bar{K} \cap \bar{\sigma} \neq \emptyset} \frac{C_{\mathbf{w},K}^2}{c_{\mathbf{w},r,K}}, \max_{K: \bar{K} \cap \bar{\sigma} \neq \emptyset} \frac{h_K^2 C_{\mathbf{w},K}^2}{c_{S,K}} \right\}.$$

Define the global and local errors, e_h and \mathcal{E}_K , of the stress and displacement variables as

$$e_h^2 := \sum_{K \in \mathcal{T}_h} \mathcal{E}_K^2, \quad \mathcal{E}_K^2 := \|S^{-1/2}(\mathbf{u} - \mathbf{u}_h)\|_K^2 + c_{\mathbf{w},r,K} \|p - p_h\|_K^2. \quad (2.5)$$

From [21], or [22] but with different forms of D_K and D_σ , it holds an upper bound estimate

$$e_h^2 \leq C_1 \eta_h^2 := C_1 \eta_{\mathcal{T}_h}^2(\mathbf{u}_h, p_h, \mathcal{T}_h) := C_1 \sum_{K \in \mathcal{T}_h} \eta_{\mathcal{T}_h}^2(\mathbf{u}_h, p_h, K), \quad (2.6)$$

where the positive constant C_1 depends only on the shape regularity of the meshes.

For a given triangulation \mathcal{T}_h and a pair of corresponding discrete solutions $(\mathbf{u}_h, p_h) \in RT_0(\mathcal{T}_h) \times P_0(\mathcal{T}_h)$, we assume that the module ESTIMATE outputs the indicators

$$\{\eta_{\mathcal{T}_h}^2(\mathbf{u}_h, p_h, K)\}_{K \in \mathcal{T}_h} = \text{ESTIMATE}(\mathbf{u}_h, p_h, \mathcal{T}_h).$$

Let \bar{R}_K denote the mean of R_K over each element $K \in \mathcal{T}_h$. We define the oscillation

$$\text{osc}_h^2 := \sum_{K \in \mathcal{T}_h} h_K^2 \|R_K - \bar{R}_K\|_K^2. \quad (2.7)$$

We note that throughout this paper the triangulation \mathcal{T}_h means a refinement of \mathcal{T}_H , and all notations with respect to the mesh \mathcal{T}_H are defined similarly. We shall also use the notation $A \lesssim B$ to represent $A \leq CB$ with $C > 0$ a mesh-size independent, generic constant.

In MARK step, by Dörfler marking we select the elements to mark according to the indicators, namely, given a grid \mathcal{T}_H with the set of indicators $\{\eta_{\mathcal{T}_H}^2(\mathbf{u}_H, p_H, K)\}_{K \in \mathcal{T}_H}$ and marking parameter $\theta \in (0, 1]$, the module MARK outputs a subset of marking elements, $\mathcal{M}_H \subset \mathcal{T}_H$, with

$$\mathcal{M}_H = \text{MARK}(\{\eta_{\mathcal{T}_H}^2(\mathbf{u}_H, p_H, K)\}_{K \in \mathcal{T}_H}, \mathcal{T}_H, \theta)$$

satisfying Dörfler property

$$\eta_{\mathcal{T}_H}(\mathbf{u}_H, p_H, \mathcal{M}_H) := \left(\sum_{K \in \mathcal{M}_H} \eta_{\mathcal{T}_H}^2(\mathbf{u}_H, p_H, K) \right)^{1/2} \geq \theta \eta_{\mathcal{T}_H}(\mathbf{u}_H, p_H, \mathcal{T}_H).$$

In REFINE step, we suppose that the refinement rule, such as the longest edge bisection [33, 34] or the newest vertex bisection [37, 28, 29], is guaranteed to produce conforming and shape regular meshes. Given a fixed integer $b \geq 1$, a mesh \mathcal{T}_H , and a subset $\mathcal{M}_H \subset \mathcal{T}_H$ of marked elements, a conforming triangulation \mathcal{T}_h is output by

$$\mathcal{T}_h = \text{REFINE}(\mathcal{T}_H, \mathcal{M}_H),$$

where all elements of \mathcal{M}_H are at least bisected b times. Note that not only marked elements get refined but also additional elements are refined to recover the conformity of triangulations.

We now describe the AMFEM algorithm. In doing so, we replace the subscript H by an iteration counter called $k \geq 0$. Let \mathcal{T}_0 be a uniform triangulation with a marking parameter $\theta \in (0, 1]$. The basic loop of AMFEM is then given by the following iterations:

<p>AMFEM algorithm</p> <p>Set $k = 0$ and iterate</p> <p>(1) $(\mathbf{u}_k, p_k) = \text{SOLVE}(\mathcal{T}_k)$;</p> <p>(2) $\{\eta_k^2(\mathbf{u}_k, p_k, K)\}_{K \in \mathcal{T}_k} = \text{ESTIMATE}(\mathbf{u}_k, p_k, \mathcal{T}_k)$;</p> <p>(3) $\mathcal{M}_k = \text{MARK}(\{\eta_k^2(\mathbf{u}_k, p_k, K)\}_{K \in \mathcal{T}_k}, \mathcal{T}_k, \theta)$;</p> <p>(4) $\mathcal{T}_{k+1} = \text{REFINE}(\mathcal{T}_k, \mathcal{M}_k)$; $k = k + 1$.</p>
--

We note that the AMFEM algorithm is a standard one in which it employs only the error estimator $\{\eta_{\mathcal{T}_k}^2(\mathbf{u}_k, p_k, K)\}_{K \in \mathcal{T}_k}$ and needs neither marking the oscillation nor the interior node property.

3. Estimate for L^2 -projection of the displacement. This section is devoted to the estimation of $\|Q_h p - p_h\|$, where Q_h is the L^2 -projection operator onto $P_0(\mathcal{T}_h)$. The estimate is one key to the proof of convergence without the quasi-orthogonality available due to the convection term. It gives as well a posteriori error estimates for the L^2 -projection of the displacement variable (see remark 3.1).

Consider the following auxiliary problem:

$$\begin{cases} \nabla \cdot (S \nabla \phi) + \nabla \phi \cdot \mathbf{w} - r \phi = Q_h p - p_h & \text{in } \Omega, \\ \phi = 0 & \text{on } \partial \Omega. \end{cases} \quad (3.1)$$

It is well known that there exists a unique solution $\phi \in H_0^1(\Omega)$ to the problem (3.1) when the convection and reaction terms satisfy $r + 1/2\nabla \cdot \mathbf{w} \geq 0$ (Assumptions (D1) and (D4)) with the following regularity estimate:

$$\|\phi\|_{H^1} = \|\phi\|_{H^1(\cup \mathcal{T}_h)} \lesssim \|Q_h p - p_h\|. \quad (3.2)$$

Moreover, if Ω is convex, $S \in C^{1,0}(\Omega)$ implies the estimate

$$\|\phi\|_{H^2(\cup \mathcal{T}_h)} \lesssim \|Q_h p - p_h\|. \quad (3.3)$$

We emphasize that we only need an estimate on $\|\phi\|_{H^2(K)}$ for each $K \in \mathcal{T}_h$, i.e., the assumption on S could be weakened in the sense that only (3.3) is required. In [9] Carstensen gave an example which shows that when S is piecewise constant, ϕ satisfies (3.3) but is not H^2 -regular.

Set $\mathbf{z} := S\nabla\phi \in H(\operatorname{div}, \Omega)$, and denote ϕ_h the L^2 -projection of ϕ onto $P_0(\mathcal{T}_h)$, and Π_h the interpolation operator from $H(\operatorname{div}, \Omega)$ onto $RT_0(\mathcal{T}_h)$ with the following estimate:

$$\|h^{-1}(\mathbf{z} - \Pi_h \mathbf{z})\| \lesssim |\mathbf{z}|_{H^1(\cup \mathcal{T}_h)} \quad \text{for all } \mathbf{z} \in H(\operatorname{div}, \Omega). \quad (3.4)$$

We refer to [2, 7, 25] for the detailed construction of such an interpolation operator Π_h and the approximation property.

From (2.1) and (2.3), we obtain

$$(Q_h p - p_h, \nabla \cdot \Pi_h \mathbf{z}) = (p - p_h, \nabla \cdot \Pi_h \mathbf{z}) = (S^{-1}(\mathbf{u} - \mathbf{u}_h), \Pi_h \mathbf{z}). \quad (3.5)$$

An integration by parts implies

$$(S^{-1}(\mathbf{u} - \mathbf{u}_h), \mathbf{z}) = (S^{-1}(\mathbf{u} - \mathbf{u}_h), S\nabla\phi) = -(\nabla \cdot (\mathbf{u} - \mathbf{u}_h), \phi). \quad (3.6)$$

From (2.2) and (2.4) it follows

$$\begin{aligned} (\nabla \cdot (\mathbf{u} - \mathbf{u}_h), \phi_h) &= (S^{-1}(\mathbf{u} - \mathbf{u}_h) \cdot \mathbf{w}, \phi_h) - ((r + \nabla \cdot \mathbf{w})(p - p_h), \phi_h) \\ &= (S^{-1}(\mathbf{u} - \mathbf{u}_h) \cdot \mathbf{w}, \phi_h) - (p - p_h, (r + \nabla \cdot \mathbf{w})\phi_h) \\ &= (S^{-1}(\mathbf{u} - \mathbf{u}_h) \cdot \mathbf{w}, \phi_h) - (Q_h p - p_h, (r + \nabla \cdot \mathbf{w})\phi_h). \end{aligned} \quad (3.7)$$

Denote $I := (Q_h(\nabla\phi \cdot \mathbf{w}), Q_h p - p_h) - (r\phi_h, Q_h p - p_h)$. In view of the commuting property of the interpolation operator Π_h , a combination of (3.5)-(3.7) yields

$$\begin{aligned} \|Q_h p - p_h\|^2 &= (Q_h p - p_h, Q_h \nabla \cdot \mathbf{z}) + I = (Q_h p - p_h, \nabla \cdot \Pi_h \mathbf{z}) + I \\ &= (S^{-1}(\mathbf{u} - \mathbf{u}_h), \Pi_h \mathbf{z} - \mathbf{z}) + (S^{-1}(\mathbf{u} - \mathbf{u}_h), \mathbf{z}) + I \\ &= (S^{-1}(\mathbf{u} - \mathbf{u}_h), \Pi_h \mathbf{z} - \mathbf{z}) - (\nabla \cdot (\mathbf{u} - \mathbf{u}_h), \phi - \phi_h) - (\nabla \cdot (\mathbf{u} - \mathbf{u}_h), \phi_h) + I \\ &= (S^{-1}(\mathbf{u} - \mathbf{u}_h), \Pi_h \mathbf{z} - \mathbf{z}) - (\nabla \cdot (\mathbf{u} - \mathbf{u}_h), \phi - \phi_h) - (S^{-1}(\mathbf{u} - \mathbf{u}_h) \cdot \mathbf{w}, \phi_h) \\ &\quad + (\nabla \cdot \mathbf{w}\phi_h, Q_h p - p_h) + (Q_h(\nabla\phi \cdot \mathbf{w}), Q_h p - p_h) \\ &= (S^{-1}(\mathbf{u} - \mathbf{u}_h), \Pi_h \mathbf{z} - \mathbf{z}) - (\nabla \cdot (\mathbf{u} - \mathbf{u}_h), \phi - \phi_h) - (S^{-1}(\mathbf{u} - \mathbf{u}_h) \cdot \mathbf{w}, \phi_h - \phi) \\ &\quad - (S^{-1}(\mathbf{u} - \mathbf{u}_h) \cdot \mathbf{w}, \phi) + (\nabla \cdot \mathbf{w}\phi_h, Q_h p - p_h) + (Q_h(\nabla\phi \cdot \mathbf{w}), Q_h p - p_h). \end{aligned} \quad (3.8)$$

Recall the postprocessed technique developed by Vohralík in [39], where a postprocessed approximation \tilde{p}_h to the displacement p is constructed such that $-S_K \nabla \tilde{p}_h|_K = \mathbf{u}_h$ and

$\frac{1}{|K|} \int_K \tilde{p}_h d\mathbf{x} = p_h|_K$ for all $K \in \mathcal{T}_h$. Then, from $\mathbf{w} \in RT_0(\mathcal{T}_h)$, we have

$$\begin{aligned}
-(S^{-1}(\mathbf{u} - \mathbf{u}_h) \cdot \mathbf{w}, \phi) &= \sum_{K \in \mathcal{T}_h} \int_K \nabla(p - \tilde{p}_h) \cdot \mathbf{w} \phi \\
&= \sum_{K \in \mathcal{T}_h} \int_K \nabla \cdot ((p - \tilde{p}_h) \mathbf{w}) \phi - \nabla \cdot \mathbf{w} (p - \tilde{p}_h) \phi \\
&= \sum_{K \in \mathcal{T}_h} \int_K -\nabla \phi \cdot \mathbf{w} (p - \tilde{p}_h) + \int_{\partial K} (p - \tilde{p}_h) \mathbf{w} \cdot \mathbf{n} \phi - (\nabla \cdot \mathbf{w} \phi, p - \tilde{p}_h) \\
&= -(\nabla \phi \cdot \mathbf{w}, p - \tilde{p}_h) - (\nabla \cdot \mathbf{w} \phi, p - \tilde{p}_h) - \sum_{\sigma \in \varepsilon_h^0} \int_{\sigma} [\tilde{p}_h] \mathbf{w} \cdot \mathbf{n} \phi.
\end{aligned} \tag{3.9}$$

Notice that it holds

$$(Q_h(\nabla \phi \cdot \mathbf{w}), Q_h p - p_h) = (Q_h(\nabla \phi \cdot \mathbf{w}), p - p_h) = (Q_h(\nabla \phi \cdot \mathbf{w}), p - \tilde{p}_h) \tag{3.10}$$

and

$$(\nabla \cdot \mathbf{w} \phi_h, Q_h p - p_h) = (\nabla \cdot \mathbf{w} \phi_h, p - p_h) = (\nabla \cdot \mathbf{w} \phi_h, p - \tilde{p}_h). \tag{3.11}$$

For convenience, denote

$$\begin{aligned}
I_1 &:= (S^{-1}(\mathbf{u} - \mathbf{u}_h), \Pi_h \mathbf{z} - \mathbf{z}), \quad I_2 := -(\nabla \cdot (\mathbf{u} - \mathbf{u}_h), \phi - \phi_h), \\
I_3 &:= -(S^{-1}(\mathbf{u} - \mathbf{u}_h) \cdot \mathbf{w}, \phi_h - \phi), \quad I_4 := -(\nabla \phi \cdot \mathbf{w} - Q_h(\nabla \phi \cdot \mathbf{w}), p - \tilde{p}_h), \\
I_5 &:= -(\nabla \cdot \mathbf{w}(\phi - \phi_h), p - \tilde{p}_h), \quad I_6 := -\sum_{\sigma \in \varepsilon_h^0} \int_{\sigma} [\tilde{p}_h] \mathbf{w} \cdot \mathbf{n} \phi.
\end{aligned}$$

From (3.8)-(3.11) we arrive at

$$\begin{aligned}
\|Q_h p - p_h\|^2 &= \sum_{i=1}^4 I_i - (\nabla \cdot \mathbf{w} \phi, p - \tilde{p}_h) + (\nabla \cdot \mathbf{w} \phi_h, Q_h p - p_h) + I_6 \\
&= \sum_{i=1}^4 I_i - (\nabla \cdot \mathbf{w}(\phi - \phi_h), p - \tilde{p}_h) - (\nabla \cdot \mathbf{w} \phi_h, p - \tilde{p}_h) \\
&\quad + (\nabla \cdot \mathbf{w} \phi_h, Q_h p - p_h) + I_6 = \sum_{i=1}^6 I_i.
\end{aligned} \tag{3.12}$$

In what follows, we separately estimate $I_i, i = 1, \dots, 6$.

LEMMA 3.1. *Denote $\|h\|_{L^\infty(\Omega)}$ the maximum norm of the mesh-size function h with respect to \mathcal{T}_h , e_h the error defined in (2.5). Then it holds*

$$I_1 \lesssim \|h\|_{L^\infty(\Omega)} e_h \|Q_h p - p_h\|. \tag{3.13}$$

Proof. From (3.4) and (3.3) it follows

$$\begin{aligned}
I_1 &= \sum_{K \in \mathcal{T}_h} (S^{-1}(\mathbf{u} - \mathbf{u}_h), \Pi_h \mathbf{z} - \mathbf{z})_K \\
&\lesssim \sum_{K \in \mathcal{T}_h} \|S^{-1/2}(\mathbf{u} - \mathbf{u}_h)\|_K \|\Pi_h \mathbf{z} - \mathbf{z}\|_K \\
&\lesssim \|h\|_{L^\infty(\Omega)} e_h |\mathbf{z}|_{H^1(\cup \mathcal{T}_h)} \\
&\lesssim \|h\|_{L^\infty(\Omega)} e_h \|Q_h p - p_h\|.
\end{aligned} \tag{3.14}$$

□

LEMMA 3.2. *It holds*

$$I_2 \lesssim (\|h\|_{L^\infty(\Omega)} e_h + \text{osc}_h) \|Q_h p - p_h\|. \tag{3.15}$$

Proof. Notice that (2.2) can be equivalently written as:

$$(\nabla \cdot \mathbf{u}, \varphi)_K - (S^{-1} \mathbf{u} \cdot \mathbf{w}, \varphi)_K + ((r + \nabla \cdot \mathbf{w})p, \varphi)_K = (f, \varphi)_K \quad \text{for all } \varphi \in L^2(K), K \in \mathcal{T}_h. \tag{3.16}$$

Meanwhile, the relation (2.4) can be equivalently written as:

$$(\nabla \cdot \mathbf{u}_h, \varphi)_K - (S^{-1} \mathbf{u}_h \cdot \mathbf{w}, \varphi)_K + ((r + \nabla \cdot \mathbf{w})p_h, \varphi)_K = (f, \varphi)_K \quad \text{for all } \varphi \in P_0(K), K \in \mathcal{T}_h. \tag{3.17}$$

For arbitrary $\varphi \in L^2(K)$, let $\bar{\varphi}_K$ denote the mean of φ over $K \in \mathcal{T}_h$. A combination of (3.16) and (3.17) yields

$$\begin{aligned}
&(\nabla \cdot (\mathbf{u} - \mathbf{u}_h), \varphi)_K = (\nabla \cdot \mathbf{u}, \varphi)_K - (\nabla \cdot \mathbf{u}_h, \varphi - \bar{\varphi}_K)_K - (\nabla \cdot \mathbf{u}_h, \bar{\varphi}_K)_K \\
&= (R_K, \varphi - \bar{\varphi}_K)_K + (S^{-1}(\mathbf{u} - \mathbf{u}_h) \cdot \mathbf{w}, \varphi)_K - ((r + \nabla \cdot \mathbf{w})(p - p_h), \varphi)_K \\
&= (R_K - \bar{R}_K, \varphi - \bar{\varphi}_K)_K + (S^{-1}(\mathbf{u} - \mathbf{u}_h) \cdot \mathbf{w}, \varphi)_K - ((r + \nabla \cdot \mathbf{w})(p - p_h), \varphi)_K \\
&\leq (\|R_K - \bar{R}_K\|_K + \|S^{-1}(\mathbf{u} - \mathbf{u}_h)\|_K \|\mathbf{w}\|_{L^\infty(K)} + C_{\mathbf{w}, r, K} \|p - p_h\|_K) \|\varphi\|_K.
\end{aligned}$$

Here we recall that \bar{R}_K is the mean of the elementwise residual R_K over each $K \in \mathcal{T}_h$. The above inequality indicates

$$\begin{aligned}
\|\nabla \cdot (\mathbf{u} - \mathbf{u}_h)\|_K &= \sup_{\varphi \in L^2(K), \varphi \neq 0} \frac{(\nabla \cdot (\mathbf{u} - \mathbf{u}_h), \varphi)_K}{\|\varphi\|_{L^2(K)}} \\
&\lesssim \|R_K - \bar{R}_K\|_K + \mathcal{E}_K.
\end{aligned} \tag{3.18}$$

Then it follows

$$\begin{aligned}
I_2 &= - \sum_{K \in \mathcal{T}_h} (\nabla \cdot (\mathbf{u} - \mathbf{u}_h), \phi - \phi_h) \\
&\lesssim \sum_{K \in \mathcal{T}_h} \|\nabla \cdot (\mathbf{u} - \mathbf{u}_h)\|_K h_K \|\nabla \phi\|_K \\
&\lesssim (\|h\|_{L^\infty(\Omega)} e_h + \text{osc}_h) \|\nabla \phi\|.
\end{aligned} \tag{3.19}$$

The desired result (3.15) follows from (3.19) and (3.2). □

LEMMA 3.3. *It holds*

$$I_3 \lesssim \|h\|_{L^\infty(\Omega)} e_h \|Q_h p - p_h\|. \quad (3.20)$$

Proof. By noticing

$$\begin{aligned} I_3 &= - \sum_{K \in \mathcal{T}_h} (S^{-1}(\mathbf{u} - \mathbf{u}_h) \cdot \mathbf{w}, \phi_h - \phi)_K \\ &\lesssim \sum_{K \in \mathcal{T}_h} \|S^{-1/2}(\mathbf{u} - \mathbf{u}_h)\|_K h_K \|\nabla \phi\|_K \\ &\leq \|h\|_{L^\infty(\Omega)} e_h \|\phi\|_{H^1} \end{aligned} \quad (3.21)$$

the desired result (3.20) follows from (3.21) and the regularity estimate (3.2). \square

LEMMA 3.4. *It holds*

$$I_4 \lesssim \|h\|_{L^\infty(\Omega)} e_h \|Q_h p - p_h\|. \quad (3.22)$$

Proof. Recall a local efficiency estimate of $h_K \|S^{-1} \mathbf{u}_h\|_K$ as following (see Lemma 7.3 in [21, 22]):

$$h_K \|S^{-1} \mathbf{u}_h\|_K \lesssim \mathcal{E}_K. \quad (3.23)$$

By triangle inequality we obtain

$$\begin{aligned} I_4 &= - \sum_{K \in \mathcal{T}_h} (\nabla \phi \cdot \mathbf{w} - Q_h(\nabla \phi \cdot \mathbf{w}), p - \tilde{p}_h)_K \\ &\lesssim \sum_{K \in \mathcal{T}_h} h_K \|\nabla(\nabla \phi \cdot \mathbf{w})\|_K (\|p - p_h\|_K + \|p_h - \tilde{p}_h\|_K) \\ &\lesssim \sum_{K \in \mathcal{T}_h} h_K \|\phi\|_{H^2(K)} (\|p - p_h\|_K + h_K \|S^{-1} \mathbf{u}_h\|_K). \end{aligned} \quad (3.24)$$

From (3.23) it holds

$$\|p - p_h\|_K + h_K \|S^{-1} \mathbf{u}_h\|_K \lesssim \mathcal{E}_K. \quad (3.25)$$

According to (3.24) and (3.25), we arrive at

$$I_4 \lesssim \sum_{K \in \mathcal{T}_h} h_K \|\phi\|_{H^2(K)} \mathcal{E}_K,$$

which, together with the regularity estimate (3.3) of ϕ , implies the result (3.22). \square

LEMMA 3.5. *It holds*

$$I_5 \lesssim e_h \|h\|_{L^\infty(\Omega)} \|Q_h p - p_h\|. \quad (3.26)$$

Proof. From (3.25) it follows

$$\begin{aligned}
I_5 &= - \sum_{K \in \mathcal{T}_h} (\nabla \cdot \mathbf{w}(\phi - \phi_h), p - \tilde{p}_h)_K \\
&\lesssim \sum_{K \in \mathcal{T}_h} \|\phi - \phi_h\|_K (\|p - p_h\|_K + \|p_h - \tilde{p}_h\|_K) \\
&\lesssim \sum_{K \in \mathcal{T}_h} h_K \|\nabla \phi\|_K (\|p - p_h\|_K + h_K \|S^{-1} \mathbf{u}_h\|_K) \\
&\lesssim e_h \|h\|_{L^\infty(\Omega)} \|\phi\|_{H^1},
\end{aligned}$$

which, together with (3.2), yields the estimate (3.26). \square

LEMMA 3.6. *It holds*

$$I_6 \lesssim e_h \|h\|_{L^\infty(\Omega)}^{1/2} \|Q_h p - p_h\|. \quad (3.27)$$

Proof. For any $\sigma \in \varepsilon_h^0$, let ϕ_σ denote the mean of ϕ onto σ , i.e., $\phi_\sigma := \frac{1}{|\sigma|} \int_\sigma \phi ds$. According to the continuity of the means of traces of the postprocessed scalar \tilde{p}_h (see Lemma 6.1 in [39]), and noticing $\mathbf{w} \in RT_0(\mathcal{T}_h)$, we have

$$\begin{aligned}
\int_\sigma [\tilde{p}_h] \mathbf{w} \cdot \mathbf{n} \phi &= \int_\sigma [\tilde{p}_h] \mathbf{w} \cdot \mathbf{n} (\phi - \phi_\sigma) \\
&\lesssim \|[\tilde{p}_h]\|_\sigma \|\phi - \phi_\sigma\|_\sigma.
\end{aligned} \quad (3.28)$$

A sidewise Poincaré inequality and trace theory imply

$$\|\phi - \phi_\sigma\|_\sigma \lesssim h_\sigma \|\gamma_{\mathbf{t}_\sigma}(\nabla \phi)\|_\sigma \lesssim h_\sigma \|\phi\|_{H^2(\cup \omega_\sigma)}. \quad (3.29)$$

From trace theorem, generalized Friedrichs inequality (see (2.2) in [39]), and the post-processed technique, we have

$$\|[\tilde{p}_h]\|_\sigma = \|[\tilde{p}_h] - \frac{1}{|\sigma|} \int_\sigma [\tilde{p}_h] ds\|_\sigma \lesssim h_\sigma^{1/2} \|\nabla_h \tilde{p}_h\|_{\omega_\sigma} \leq h_\sigma^{1/2} \|S^{-1} \mathbf{u}_h\|_{\omega_\sigma}. \quad (3.30)$$

A combination of (3.28)-(3.30) yields

$$\int_\sigma [\tilde{p}_h] \mathbf{w} \cdot \mathbf{n} \phi \lesssim h_\sigma \|S^{-1} \mathbf{u}_h\|_{\omega_\sigma} h_\sigma^{1/2} \|\phi\|_{H^2(\cup \omega_\sigma)}. \quad (3.31)$$

In light of the local shape regularity of element, the above estimate leads to

$$\begin{aligned}
I_6 &\lesssim \sum_{\sigma \in \varepsilon_h^0} h_\sigma \|S^{-1} \mathbf{u}_h\|_{\omega_\sigma} h_\sigma^{1/2} \|\phi\|_{H^2(\cup \omega_\sigma)} \\
&\lesssim \|h\|_{L^\infty(\Omega)}^{1/2} \left(\sum_{K \in \mathcal{T}_h} h_K^2 \|S^{-1} \mathbf{u}_h\|_K^2 \right)^{1/2} \|\phi\|_{H^2(\cup \mathcal{T}_h)}.
\end{aligned} \quad (3.32)$$

The desired result (3.27) follows from (3.32), (3.23) and (3.3). \square

We now give an estimate of $\|Q_h p - p_h\|$.

THEOREM 3.7. *Let e_h , osc_h , and $\|h\|_{L^\infty(\Omega)}$ denote the error of the stress and displacement variables given in (2.5), the oscillation of data given in (2.7), and the maximum norm*

of the mesh-size function, respectively, with respect to \mathcal{T}_h . Then there exists a positive constant C_2 only depending on the shape regularity of \mathcal{T}_h , such that

$$\|Q_h p - p_h\| \leq C_2 C_D (\|h\|_{L^\infty(\Omega)}^{1/2} e_h + \text{osc}_h), \quad (3.33)$$

where C_D is one variant of coefficients.

Proof. The estimate (3.33) follows from a combination of (3.12), (3.13), (3.15), (3.20), (3.22), (3.26), and (3.27). \square

REMARK 3.1. A combination of the two estimates (3.33) and (2.6) actually give a posteriori bound for $Q_h(p - p_h)$. Furthermore, following [7], we denote

$$\mathcal{L}_k^{1,NC} := \{q_h \in L^2(\Omega) : q_h|_K \in P_k(K), \forall K \in \mathcal{T}_h, \sum_K \int_{\partial K} p_h \phi ds = 0, \forall \phi \in \mathcal{R}_k(\partial K)\},$$

and let p_h^*, \hat{p}_h be respectively the interpolates in $\mathcal{L}_k^{1,NC}$ of the interelement Lagrangian multiplier λ_h and the displacement p ([7], pages 186-187; We note that in [7] u represents the displacement variable and p the stress variable). Following the same line as in [7], it holds the estimate

$$\|\hat{p}_h - p_h^*\| \lesssim \|hS^{-1/2}(\mathbf{u} - \mathbf{u}_h)\| + \|Q_h(p - p_h)\|,$$

which gives an a posteriori error estimate for $\hat{p}_h - p_h^*$.

REMARK 3.2. For a pure diffusion problem, i.e., $\mathbf{w} = r = 0$ in (1.1), it holds $I_i = 0, i = 3, 4, 5, 6$. From the estimates of I_1 and I_2 , we can obtain

$$\|Q_h p - p_h\| \lesssim \|hS^{-1/2}(\mathbf{u} - \mathbf{u}_h)\| + \text{osc}_h,$$

which results in the quasi-orthogonality

$$(S^{-1}(\mathbf{u} - \mathbf{u}_h), \mathbf{u}_h - \mathbf{u}_H) \lesssim (\|hS^{-1/2}(\mathbf{u} - \mathbf{u}_h)\| + \text{osc}_h) \|f_h - f_H\|,$$

where we have used the fact that $\nabla \cdot \mathbf{u}_h = Q_h f = f_h$ and $\nabla \cdot \mathbf{u}_H = Q_H f = f_H$. This estimate is somewhat different from the quasi-orthogonality results in [10, 13, 14, 19, 20].

4. Estimator reduction. Let ω_σ denote the patch of $\sigma \in \varepsilon_h$, and define $c_{\omega_\sigma}, D_{\omega_K}^2, D_{\mathcal{T}_h}^2(K), D_{\mathcal{T}_h}^2$ respectively by

$$c_{\omega_\sigma} := \begin{cases} \max(c_{S,K}^{-1/2}, c_{S,L}^{-1/2}) & \text{if } \sigma = K \cap L, \\ c_{S,K}^{-1/2} & \text{if } \sigma \in \varepsilon_K \cap \partial\Omega, \end{cases} \quad D_{\omega_K}^2 := \max_{\sigma \in \varepsilon_K} D_\sigma^2 c_{\omega_\sigma}^2,$$

$$D_{\mathcal{T}_h}^2(K) := \max(h_K^2 D_K^2 c_{S,K}^{-1}, C_{DK} \alpha_K^2, D_{\omega_K}^2), \quad D_{\mathcal{T}_h}^2 := \sum_{K \in \mathcal{T}_h} D_{\mathcal{T}_h}^2(K),$$

where C_{DK} in $D_{\mathcal{T}_h}^2(K)$ is given by

$$C_{DK} := 2 \max\left(\left(C_4 C_{S,K}^{1/2} + \frac{h_K}{\sqrt{c_{S,K}}}\|\mathbf{w}\|_{L^\infty(K)}\right)^2, \frac{h_K^2 C_{\mathbf{w},r,K}^2}{c_{\mathbf{w},r,K}}\right).$$

LEMMA 4.1. (Estimator reduction) For a triangulation \mathcal{T}_H with $\mathcal{M}_H \subset \mathcal{T}_H$, let \mathcal{T}_h be a refinement of \mathcal{T}_H obtained by the AMFEM algorithm. Denote by $D_{\mathcal{T}_0}^2$ one variant of the coefficients onto the initial mesh \mathcal{T}_0 , and denote $\lambda := 1 - 2^{-b/2}$,

$$E_H^2 := \sum_{K \in \mathcal{T}_h} \|S^{-1/2}(\mathbf{u}_h - \mathbf{u}_H)\|_K^2 + c_{\mathbf{w},r,K} \|p_h - p_H\|_K^2. \quad (4.1)$$

Then for any $0 < \delta < 1$, it holds

$$\eta_{\mathcal{T}_h}^2(\mathbf{u}_h, p_h, \mathcal{T}_h) \leq (1+\delta)\{\eta_{\mathcal{T}_H}^2(\mathbf{u}_H, p_H, \mathcal{T}_H) - \lambda\eta_{\mathcal{T}_H}^2(\mathbf{u}_H, p_H, \mathcal{M}_H)\} + C_3^2(1+\delta^{-1})D_{\mathcal{T}_0}^2 E_H^2. \quad (4.2)$$

Proof. By triangle inequality and Young inequality, we have

$$h_K^2 \|S^{-1}\mathbf{u}_h\|_K^2 \leq (1+\delta)h_K^2 \|S^{-1}\mathbf{u}_H\|_K^2 + (1+\delta^{-1})h_K^2 c_{S,K}^{-1} \|S^{-1/2}(\mathbf{u}_h - \mathbf{u}_H)\|_K^2. \quad (4.3)$$

Inverse inequality implies

$$\|\nabla \cdot (\mathbf{u}_h - \mathbf{u}_H)\|_K \leq C_4 C_{S,K}^{1/2} h_K^{-1} \|S^{-1/2}(\mathbf{u}_h - \mathbf{u}_H)\|_K,$$

which leads to

$$\begin{aligned} & h_K^2 \|f - \nabla \cdot \mathbf{u}_h + S^{-1}\mathbf{u}_h \cdot \mathbf{w} - (r + \nabla \cdot \mathbf{w})p_h\|_K^2 \\ & \leq (1+\delta)h_K^2 \|f - \nabla \cdot \mathbf{u}_H + S^{-1}\mathbf{u}_H \cdot \mathbf{w} - (r + \nabla \cdot \mathbf{w})p_H\|_K^2 \\ & \quad + (1+\delta^{-1})C_{DK} (\|S^{-1/2}(\mathbf{u}_h - \mathbf{u}_H)\|_K^2 + c_{\mathbf{w},r,K} \|p_h - p_H\|_K^2). \end{aligned} \quad (4.4)$$

From inverse inequality and local shape regularity of the mesh, it follows

$$\|[\gamma_{\mathbf{t}_\sigma}(S^{-1}\mathbf{u}_h)]\|_\sigma \leq \|[\gamma_{\mathbf{t}_\sigma}(S^{-1}\mathbf{u}_H)]\|_\sigma + C_5 c_{\omega_\sigma} h_\sigma^{-1/2} \|S^{-1/2}(\mathbf{u}_h - \mathbf{u}_H)\|_{\omega_\sigma}, \quad (4.5)$$

which, together with Young inequality, yields

$$h_\sigma \|[\gamma_{\mathbf{t}_\sigma}(S^{-1}\mathbf{u}_h)]\|_\sigma^2 \leq (1+\delta)h_\sigma \|[\gamma_{\mathbf{t}_\sigma}(S^{-1}\mathbf{u}_H)]\|_\sigma^2 + (1+\delta^{-1})C_5^2 c_{\omega_\sigma}^2 \|S^{-1/2}(\mathbf{u}_h - \mathbf{u}_H)\|_{\omega_\sigma}^2. \quad (4.6)$$

Summing (4.3) and (4.4) over all elements $K \in \mathcal{T}_h$, summing (4.6) over all interior sides $\sigma \in \varepsilon_h^0$, and noticing the monotonicity of variants of coefficients, we obtain

$$\eta_{\mathcal{T}_h}^2(\mathbf{u}_h, p_h, \mathcal{T}_h) \leq (1+\delta)\eta_{\mathcal{T}_h}^2(\mathbf{u}_H, p_H, \mathcal{T}_h) + C_3^2(1+\delta^{-1})D_{\mathcal{T}_h}^2 E_H^2. \quad (4.7)$$

For a marked element $K \in \mathcal{M}_H$, we set $\mathcal{T}_{h,K} := \{K' \in \mathcal{T}_h | K' \subset K\}$. It holds

$$\begin{cases} \sum_{K' \in \mathcal{T}_{h,K}} \eta_{\mathcal{T}_h}^2(\mathbf{u}_H, p_H, K') \leq 2^{-b/2} \eta_{\mathcal{T}_H}^2(\mathbf{u}_H, p_H, K) & \text{for } K \in \mathcal{T}_H / \mathcal{T}_h, \\ \eta_{\mathcal{T}_h}^2(\mathbf{u}_H, p_H, K) \leq \eta_{\mathcal{T}_H}^2(\mathbf{u}_H, p_H, K) & \text{for } K \in \mathcal{T}_H / \mathcal{M}_H, \end{cases}$$

which results in the following estimate

$$\begin{aligned} \eta_{\mathcal{T}_h}^2(\mathbf{u}_H, p_H, \mathcal{T}_h) & \leq 2^{-b/2} \eta_{\mathcal{T}_H}^2(\mathbf{u}_H, p_H, \mathcal{M}_H) + \eta_{\mathcal{T}_H}^2(\mathbf{u}_H, p_H, \mathcal{T}_H / \mathcal{T}_h) \\ & = \eta_{\mathcal{T}_H}^2(\mathbf{u}_H, p_H, \mathcal{T}_H) - \lambda \eta_{\mathcal{T}_H}^2(\mathbf{u}_H, p_H, \mathcal{M}_H). \end{aligned} \quad (4.8)$$

The desired result (4.2) follows from (4.7), (4.8) and the monotonicity of $D_{\mathcal{T}_h}$. \square

5. Proof of theorem 1.1. In this section, we show that the error plus some quantity uniformly reduces with a fixed factor on two successive meshes, which shows AMFEM is convergent.

LEMMA 5.1. *Let $(\mathbf{u}_h, p_h) \in RT_0(\mathcal{T}_h) \times P_0(\mathcal{T}_h)$ be the approximation solutions to the stress and displacement variables with respect to \mathcal{T}_h , and e_h the error of the stress and displacement variables with respect to \mathcal{T}_h . Denote by h_0 the mesh-size of the quasi-uniform*

initial mesh \mathcal{T}_0 , by D_1 one variant of the coefficients determined by C_D . Then it holds for any $0 < \delta_1 < 1$

$$\begin{aligned} \|S^{-1/2}(\mathbf{u} - \mathbf{u}_h)\|^2 &\leq 2\delta_1^{-1}D_1(h_0e_h^2 + h_0^2(\|f - f_h\|^2 + \|h\nabla_h(S^{-1}\mathbf{u}_h \cdot \mathbf{w})\|^2)) \\ &\quad + \|S^{-1/2}(\mathbf{u} - \mathbf{u}_H)\|^2 - \|S^{-1/2}(\mathbf{u}_h - \mathbf{u}_H)\|^2 + 1/2\delta_1\|\nabla \cdot (\mathbf{u}_h - \mathbf{u}_H)\|^2. \end{aligned} \quad (5.1)$$

Proof. From (2.1) and (2.3) we get

$$\begin{aligned} \|S^{-1/2}(\mathbf{u} - \mathbf{u}_h)\|^2 &= \|S^{-1/2}(\mathbf{u} - \mathbf{u}_H)\|^2 - \|S^{-1/2}(\mathbf{u}_h - \mathbf{u}_H)\|^2 \\ &\quad - 2(S^{-1}(\mathbf{u} - \mathbf{u}_h), \mathbf{u}_h - \mathbf{u}_H) \\ &= \|S^{-1/2}(\mathbf{u} - \mathbf{u}_H)\|^2 - \|S^{-1/2}(\mathbf{u}_h - \mathbf{u}_H)\|^2 \\ &\quad - 2(p - p_h, \nabla \cdot (\mathbf{u}_h - \mathbf{u}_H)) \\ &= \|S^{-1/2}(\mathbf{u} - \mathbf{u}_H)\|^2 - \|S^{-1/2}(\mathbf{u}_h - \mathbf{u}_H)\|^2 \\ &\quad - 2(Q_h p - p_h, \nabla \cdot (\mathbf{u}_h - \mathbf{u}_H)). \end{aligned} \quad (5.2)$$

The definition of the residual R_K and the assumptions of data imply that for each $K \in \mathcal{T}_h$,

$$h_K \|R_K - \bar{R}_K\|_K \leq C_6(h_K^2 \|\nabla(S^{-1}\mathbf{u}_h \cdot \mathbf{w})\|_K + h_K \|f - f_h\|_K),$$

which, together with the fact $\|h\|_{L^\infty(\Omega)} \leq h_0$ and the definition (2.7) of osc_h , yields the estimate

$$\text{osc}_h^2 \leq 2C_6^2 h_0^2 (\|f - f_h\|^2 + \|h\nabla_h(S^{-1}\mathbf{u}_h \cdot \mathbf{w})\|^2). \quad (5.3)$$

Applying the above estimate (5.3) to (3.33), we obtain

$$\|Q_h p - p_h\|^2 \leq D_1(h_0e_h^2 + h_0^2(\|f - f_h\|^2 + \|h\nabla_h(S^{-1}\mathbf{u}_h \cdot \mathbf{w})\|^2)). \quad (5.4)$$

In light of Young inequality, we have

$$2(Q_h p - p_h, \nabla \cdot (\mathbf{u}_h - \mathbf{u}_H)) \leq 2\delta_1^{-1}\|Q_h p - p_h\|^2 + \delta_1/2\|\nabla \cdot (\mathbf{u}_h - \mathbf{u}_H)\|^2. \quad (5.5)$$

The desired result (5.1) follows from a combination of (5.2), (5.4), and (5.5). \square

LEMMA 5.2. Let D_2 and D_3 be two variants of the coefficients respectively given by

$$D_2 := \max_{K \in \mathcal{T}_h} \|\mathbf{w}\|_{L^\infty(K)}^2 c_{S,K}^{-1}, \quad D_3 := \max_{K \in \mathcal{T}_h} C_{\mathbf{w},r,K}.$$

Under the assumptions of Lemma 5.1, it holds

$$\begin{aligned} \|\nabla \cdot (\mathbf{u} - \mathbf{u}_h)\|^2 &\leq 4D_1D_3(h_0e_h^2 + h_0^2(\|f - f_h\|^2 + \|h\nabla_h(S^{-1}\mathbf{u}_h \cdot \mathbf{w})\|^2)) \\ &\quad + \|\nabla \cdot (\mathbf{u} - \mathbf{u}_H)\|^2 - 1/2\|\nabla \cdot (\mathbf{u}_h - \mathbf{u}_H)\|^2 + 4D_2\|S^{-1/2}(\mathbf{u} - \mathbf{u}_h)\|^2. \end{aligned} \quad (5.6)$$

Proof. Notice

$$\|\nabla \cdot (\mathbf{u} - \mathbf{u}_h)\|^2 = \|\nabla \cdot (\mathbf{u} - \mathbf{u}_H)\|^2 - \|\nabla \cdot (\mathbf{u}_h - \mathbf{u}_H)\|^2 - 2(\nabla \cdot (\mathbf{u} - \mathbf{u}_h), \nabla \cdot (\mathbf{u}_h - \mathbf{u}_H)). \quad (5.7)$$

A combination of (2.2) and (2.4) leads to

$$\begin{aligned} (\nabla \cdot (\mathbf{u} - \mathbf{u}_h), \nabla \cdot (\mathbf{u}_h - \mathbf{u}_H)) &= (S^{-1}(\mathbf{u} - \mathbf{u}_h) \cdot \mathbf{w}, \nabla \cdot (\mathbf{u}_h - \mathbf{u}_H)) \\ &\quad - ((r + \nabla \cdot \mathbf{w})(Q_h p - p_h), \nabla \cdot (\mathbf{u}_h - \mathbf{u}_H)) \quad (5.8) \\ &\leq 2D_2 \|S^{-1/2}(\mathbf{u} - \mathbf{u}_h)\|^2 + 2D_3 \|Q_h p - p_h\|^2 + 1/4 \|\nabla \cdot (\mathbf{u}_h - \mathbf{u}_H)\|. \end{aligned}$$

The estimate (5.6) follows from (5.7), (5.4) and (5.8). \square

LEMMA 5.3. *Let D_4 be one variant of the coefficients given by $D_4 := \max_{K \in \mathcal{T}_h} c_{\mathbf{w},r,K}$. Under the assumption of Lemma 5.1, it holds*

$$\begin{aligned} \sum_{K \in \mathcal{T}_h} c_{\mathbf{w},r,K} \|p - p_h\|^2 &\leq \sum_{K \in \mathcal{T}_H} c_{\mathbf{w},r,K} \|p - p_H\|_K^2 - 1/2 \sum_{K \in \mathcal{T}_H} c_{\mathbf{w},r,K} \|p_h - p_H\|_K^2 \\ &\quad + 2D_4 D_1 (h_0 e_h^2 + h_0^2 (\|f - f_h\|^2 + \|h \nabla_h (S^{-1} \mathbf{u}_h \cdot \mathbf{w})\|^2)). \quad (5.9) \end{aligned}$$

Proof. For each element $K \in \mathcal{T}_h$, it holds the following identity

$$\begin{aligned} \|p - p_h\|_K^2 &= \|p - p_H\|_K^2 - \|p_h - p_H\|_K^2 - 2(p - p_h, p_h - p_H)_K \\ &= \|p - p_H\|_K^2 - \|p_h - p_H\|_K^2 - 2(Q_h p - p_h, p_h - p_H)_K. \quad (5.10) \end{aligned}$$

Notice that $c_{\mathbf{w},r,K}$ does not change from \mathcal{T}_H to \mathcal{T}_h . Summing (5.10) by multiplying $c_{\mathbf{w},r,K}$ over all elements $K \in \mathcal{T}_h$, we have

$$\begin{aligned} \sum_{K \in \mathcal{T}_h} c_{\mathbf{w},r,K} \|p - p_h\|_K^2 &\leq \sum_{K \in \mathcal{T}_H} c_{\mathbf{w},r,K} \|p - p_H\|_K^2 - 1/2 \sum_{K \in \mathcal{T}_H} c_{\mathbf{w},r,K} \|p_h - p_H\|_K^2 \\ &\quad + 2D_4 \|Q_h p - p_h\|^2. \quad (5.11) \end{aligned}$$

The conclusion (5.9) follows from (5.11) and (5.4). \square

In what follows, we show the reduction of the error. To this end, set $\gamma_1, \gamma_2, \varepsilon_0$, and δ_1 to be any positive constants, which will be determined below. Introduce the following quantity:

$$A_h^2 := \delta_1 (1 - \varepsilon_0)^{-1} \|\nabla \cdot (\mathbf{u} - \mathbf{u}_h)\|^2 + \gamma_1 \eta_h^2 + \gamma_2 (\|f - f_h\|^2 + \|h \nabla_h (S^{-1} \mathbf{u}_h \cdot \mathbf{w})\|^2), \quad (5.12)$$

where f_h is the L^2 -projection of f onto $P_0(\mathcal{T}_h)$. We note that the definition of A_H is similar to A_h .

THEOREM 5.4. *Let $(\mathbf{u}_h, p_h) \in RT_0(\mathcal{T}_h) \times P_0(\mathcal{T}_h)$ and $(\mathbf{u}_H, p_H) \in RT_0(\mathcal{T}_H) \times P_0(\mathcal{T}_H)$ be the approximation solutions to the stress and displacement variables with respect to \mathcal{T}_h and \mathcal{T}_H , respectively. Denote by e_h and e_H the errors of the stress and displacement variables with respect to \mathcal{T}_h and \mathcal{T}_H , respectively. Let h_0 be the mesh-size of the quasi-uniform initial mesh \mathcal{T}_0 , and q and $\alpha \in (0, 1)$ two constants to be determined below. Then it holds*

$$e_h^2 + (1 - h_0 q) A_h^2 \leq \alpha^2 (e_H^2 + (1 - h_0 q) A_H^2) \quad (5.13)$$

when $h_0 \leq \frac{1 - \alpha^2}{1 + \alpha^2} \frac{1}{q}$.

Proof. For convenience, denote

$$D_5 := 2D_1 + 4\delta_1^2 D_1 D_3 + 2\delta_1 D_1 D_4.$$

Recalling the definition, (4.1), of E_H , a combination of (5.1), (5.6) and (5.9) indicates

$$\begin{aligned} e_h^2 + \delta_1 \|\nabla \cdot (\mathbf{u} - \mathbf{u}_h)\|^2 &\leq e_H^2 + \delta_1 \|\nabla \cdot (\mathbf{u} - \mathbf{u}_H)\|^2 - 1/2 E_H^2 + h_0 D_5 \delta_1^{-1} e_h^2 \\ &\quad + 4\delta_1 D_2 e_h^2 + D_5 \delta_1^{-1} h_0^2 (\|f - f_h\|^2 + \|h \nabla_h (S^{-1} \mathbf{u}_h \cdot \mathbf{w})\|^2). \quad (5.14) \end{aligned}$$

For a constant $\varepsilon > 0$ which will be determined below, denote $\varepsilon_0 := \frac{\varepsilon}{1+\varepsilon}$. We firstly choose δ_1 with $4\delta_1 D_2 \leq \varepsilon_0$. The reliable estimate, (2.6), of the stress and displacement variables, together with (5.14), implies

$$\begin{aligned} e_h^2 + \delta_1 \|\nabla \cdot (\mathbf{u} - \mathbf{u}_h)\|^2 &\leq e_H^2 + \delta_1 \|\nabla \cdot (\mathbf{u} - \mathbf{u}_H)\|^2 - 1/2 E_H^2 + C_1 D_5 \delta_1^{-1} h_0 \eta_h^2 \\ &\quad + \varepsilon_0 e_h^2 + D_5 \delta_1^{-1} h_0^2 (\|f - f_h\|^2 + \|h \nabla_h (S^{-1} \mathbf{u}_h \cdot \mathbf{w})\|^2), \end{aligned}$$

which results in the following inequality:

$$\begin{aligned} e_h^2 + \frac{\delta_1}{1-\varepsilon_0} \|\nabla \cdot (\mathbf{u} - \mathbf{u}_h)\|^2 &\leq (1 + \varepsilon) e_H^2 + \frac{\delta_1}{1-\varepsilon_0} \|\nabla \cdot (\mathbf{u} - \mathbf{u}_H)\|^2 - \frac{1}{2(1-\varepsilon_0)} E_H^2 \\ &\quad + \frac{C_1 D_5}{\delta_1 (1-\varepsilon_0)} h_0 \eta_h^2 + \frac{D_5}{\delta_1 (1-\varepsilon_0)} h_0^2 (\|f - f_h\|^2 + \|h \nabla_h (S^{-1} \mathbf{u}_h \cdot \mathbf{w})\|^2). \end{aligned} \quad (5.15)$$

According to triangle inequality and inverse inequality, it holds, for each $K \in \mathcal{T}_h$,

$$h_K \|\nabla (S^{-1} \mathbf{u}_h \cdot \mathbf{w})\|_K \leq h_K \|\nabla (S^{-1} \mathbf{u}_H \cdot \mathbf{w})\|_K + C_7 \|S^{-1} (\mathbf{u}_h - \mathbf{u}_H) \cdot \mathbf{w}\|_K. \quad (5.16)$$

Notice that $\|f - f_h\|_K \leq \|f - f_H\|_K$ for all $K \in \mathcal{T}_h$. For any given $\delta_3 > 0$ which will be determined below, (5.16) and Young inequality imply

$$\begin{aligned} \|f - f_h\|^2 + \|h \nabla_h (S^{-1} \mathbf{u}_h \cdot \mathbf{w})\|^2 &\leq (1 + \delta_3) (\|f - f_H\|^2 + \|H \nabla_H (S^{-1} \mathbf{u}_H \cdot \mathbf{w})\|^2) \\ &\quad + (1 + \delta_3^{-1}) C_7^2 D_2 \|S^{-1/2} (\mathbf{u}_h - \mathbf{u}_H)\|^2. \end{aligned} \quad (5.17)$$

From the definition, (5.12), of A_h^2 , the estimator reduction (4.2) with the marking strategy, the estimates (5.15) and (5.17), and the fact $\|S^{-1/2} (\mathbf{u}_h - \mathbf{u}_H)\|^2 \leq E_H^2$, it holds, for any given $\delta_2 > 0$ which will be determined below,

$$\begin{aligned} e_h^2 + A_h^2 &\leq (1 + \varepsilon) e_H^2 + \frac{\delta_1}{1-\varepsilon_0} \|\nabla \cdot (\mathbf{u} - \mathbf{u}_H)\|^2 - \frac{1}{2(1-\varepsilon_0)} E_H^2 + \frac{C_1 D_5}{\delta_1 (1-\varepsilon_0)} h_0 \eta_h^2 \\ &\quad + C_3^2 (1 + \delta_2^{-1}) D_{\gamma_0}^2 \gamma_1 E_H^2 + \gamma_1 (1 + \delta_2) (1 - \lambda \theta^2) \eta_H^2 + \gamma_2 C_7^2 D_2 (1 + \frac{1}{\delta_3}) E_H^2 \\ &\quad + \frac{D_5}{\delta_1 (1-\varepsilon_0)} h_0^2 (\|f - f_h\|^2 + \|h \nabla_h (S^{-1} \mathbf{u}_h \cdot \mathbf{w})\|^2) \\ &\quad + \gamma_2 (1 + \delta_3) (\|f - f_H\|^2 + \|H \nabla_H (S^{-1} \mathbf{u}_H \cdot \mathbf{w})\|^2). \end{aligned} \quad (5.18)$$

We next choose γ_1 and γ_2 such that

$$\gamma_1 C_3^2 (1 + \delta_2^{-1}) D_{\gamma_0}^2 = \frac{1}{4(1-\varepsilon_0)}, \quad \gamma_2 C_7^2 D_2 (1 + \delta_3^{-1}) = \frac{1}{4(1-\varepsilon_0)}.$$

Then it follows

$$\begin{aligned} e_h^2 + A_h^2 &\leq (1 + \varepsilon) e_H^2 + \frac{\delta_1}{1-\varepsilon_0} \|\nabla \cdot (\mathbf{u} - \mathbf{u}_H)\|^2 + \gamma_1 (1 + \delta_2) (1 - \lambda \theta^2) \eta_H^2 \\ &\quad + \frac{D_5}{\delta_1 (1-\varepsilon_0)} h_0^2 (\|f - f_h\|^2 + \|h \nabla_h (S^{-1} \mathbf{u}_h \cdot \mathbf{w})\|^2) + \frac{C_1 D_5}{\delta_1 (1-\varepsilon_0)} h_0 \eta_h^2 \\ &\quad + \gamma_2 (1 + \delta_3) (\|f - f_H\|^2 + \|H \nabla_H (S^{-1} \mathbf{u}_H \cdot \mathbf{w})\|^2). \end{aligned} \quad (5.19)$$

For any given $\delta_4, \delta_5 > 0$ which will be determined below, the reliable estimate (2.6) on \mathcal{T}_H , i.e. $e_H^2 \leq C_1 \eta_H^2$, and the above estimate (5.19), indicate

$$\begin{aligned} e_h^2 + A_h^2 &\leq (1 + \varepsilon - 1/2 \lambda \theta^2 \gamma_1 (1 + \delta_2) C_1^{-1}) e_H^2 + \gamma_1 (1 + \delta_2) (1 - 1/2 \lambda \theta^2) \eta_H^2 \\ &\quad + \frac{\delta_1 (1 - \delta_4)}{1 - \varepsilon_0} \|\nabla \cdot (\mathbf{u} - \mathbf{u}_H)\|^2 + \frac{D_5}{\delta_1 (1 - \varepsilon_0)} h_0^2 (\|f - f_h\|^2 + \|h \nabla_h (S^{-1} \mathbf{u}_h \cdot \mathbf{w})\|^2) \\ &\quad + \frac{C_1 D_5}{\delta_1 (1 - \varepsilon_0)} h_0 \eta_h^2 + (1 - \delta_5) \gamma_2 (1 + \delta_3) (\|f - f_H\|^2 + \|H \nabla_H (S^{-1} \mathbf{u}_H \cdot \mathbf{w})\|^2) \\ &\quad + \frac{\delta_1 \delta_4}{1 - \varepsilon_0} \|\nabla \cdot (\mathbf{u} - \mathbf{u}_H)\|^2 + (1 + \delta_3) \delta_5 \gamma_2 (\|f - f_H\|^2 + \|H \nabla_H (S^{-1} \mathbf{u}_H \cdot \mathbf{w})\|^2). \end{aligned} \quad (5.20)$$

Now we fix a sufficiently small δ_2 and, subsequently, a sufficiently small ε such that

$$\tilde{\alpha}^2 := \max\left(1 + \varepsilon - \frac{C_1}{2}\lambda\theta^2\gamma_1(1 + \delta_2), (1 + \delta_2)\left(1 - \frac{\lambda\theta^2}{2}\right), 1 - \delta_4, (1 - \delta_5)(1 + \delta_3)\right) < 1.$$

Let D_6 be one variant of the coefficients given by

$$D_6 := 4 \max_{K \in \mathcal{T}_H} (\|\mathbf{w}\|_{L^\infty(K)}^2 c_{S,K}^{-1}, C_{\mathbf{w},r,K}^2 c_{\mathbf{w},r,K}^{-1}, 1).$$

From (3.18), we get

$$\|\nabla \cdot (\mathbf{u} - \mathbf{u}_H)\|^2 \leq D_6 (\|f - f_H\|^2 + \|H\nabla_H(S^{-1}\mathbf{u}_H \cdot \mathbf{w})\|^2 + \eta_H^2). \quad (5.21)$$

We further choose δ_i ($i = 3, 4, 5$) such that

$$\frac{\delta_1\delta_4}{1 - \varepsilon_0} D_6 \leq \gamma_2 h_0, \quad (1 + \delta_3)\delta_5 \leq C_8 h_0.$$

In fact, we may firstly fix δ_3 satisfying $\delta_3 < C_8 h_0$, then choose δ_5 such that

$$\frac{\delta_3}{1 + \delta_3} < \delta_5 < \min\left(1, \frac{C_8 h_0}{1 + \delta_3}\right).$$

Finally, by noticing the choice of γ_2 , we can choose δ_4 with

$$\delta_4 < \min\left(1, \frac{h_0}{D_6} \frac{1 - \varepsilon_0}{\delta_1} \frac{1}{4C_7^2 D_2 (1 - \varepsilon_0)(1 + \delta_3^{-1})}\right).$$

These choices, together with (5.20) and (5.21), lead to

$$\begin{aligned} e_h^2 + A_h^2 &\leq \tilde{\alpha}^2 (e_H^2 + A_H^2) + \frac{C_1 D_5}{\delta_1 (1 - \varepsilon_0)} h_0 \eta_h^2 \\ &\quad + \frac{D_5}{\delta_1 (1 - \varepsilon_0)} h_0^2 (\|f - f_h\|^2 + \|h\nabla_h(S^{-1}\mathbf{u}_h \cdot \mathbf{w})\|^2) \\ &\quad + \gamma_2 h_0 (1 + C_8) (\|f - f_H\|^2 + \|H\nabla_H(S^{-1}\mathbf{u}_H \cdot \mathbf{w})\|^2) + \gamma_2 h_0 \eta_H^2. \end{aligned} \quad (5.22)$$

Let q be one variant of the coefficients given by

$$q := \max\left(C_8 + 1, \frac{\gamma_2}{\gamma_1}, \frac{C_1 D_5}{\delta_1 (1 - \varepsilon_0)} \frac{1}{\gamma_1}, \frac{D_5}{\delta_1 (1 - \varepsilon_0)} \frac{h_0}{\gamma_2}\right).$$

From (5.22) we arrive at

$$e_h^2 + A_h^2 \leq \tilde{\alpha}^2 (e_H^2 + A_H^2) + q h_0 (A_h^2 + A_H^2),$$

which implies

$$e_h^2 + (1 - q h_0) A_h^2 \leq \tilde{\alpha}^2 e_H^2 + (\tilde{\alpha}^2 + q h_0) A_H^2. \quad (5.23)$$

We finally choose h_0 such that

$$0 < \frac{\tilde{\alpha}^2 + q h_0}{1 - q h_0} \leq \alpha^2 := \frac{1 + \tilde{\alpha}^2}{2},$$

which yields the assertion (5.13) with $h_0 \leq (1 - \alpha^2)/(q(1 + \alpha^2))$. \square

REMARK 5.1. (Choices of the initial mesh size) *Some simple calculations show*

$$q \leq \max\{D(\delta_1, \delta_2), \frac{D_5 h_0 C_7^{-2}}{4\delta_1(1-\varepsilon_0)^2 D_2}\}$$

with

$$D(\delta_1, \delta_2) := \max\{C_8 + 1, \frac{C_3^2(1+\delta_2^{-1})D_{\mathcal{T}_0}^2}{C_7^2 D_2}, \frac{C_2 D_5}{4\delta_1(1-\varepsilon_0)C_3^2(1+\delta_2^{-1})D_{\mathcal{T}_0}^2}\}.$$

Then it holds

$$\frac{1}{q} \geq \min\left\{\frac{1}{D(\delta_1, \delta_2)}, \frac{4\delta_1(1-\varepsilon_0)^2 C_7^2 D_2}{D_5 h_0}\right\},$$

which indicates

$$\frac{1}{q} \geq \frac{1}{D(\delta_1, \delta_2)} \quad \text{if} \quad h_0 \leq \frac{4\delta_1(1-\varepsilon_0)^2 C_7^2 D_2}{D_5}.$$

As required in Theorem 5.4, the initial mesh size h_0 is assumed to satisfy $h_0 \leq \frac{1-\alpha^2}{q(1+\alpha^2)}$. Then eventually we may choose h_0 with

$$h_0 \leq \min\left\{\frac{1-\alpha^2}{(1+\alpha^2)D(\delta_1, \delta_2)}, \frac{4\delta_1(1-\varepsilon_0)^2 C_7^2 D_2}{D_5}\right\}.$$

The proof of Theorem 1.1 Theorem 5.4 shows that the error of the stress and displacement variables plus the quantity A_h^2 uniformly reduces with a fixed factor α^2 between two successive meshes. Replace the subscripts H and h respectively by the iteration counters k and $k+1$, we then obtain Theorem 1.1 directly from Theorem 5.4.

6. Numerical experiments. In this section, we test the performance of the adaptive algorithm AMFEM described in section 2 with four model problems. We are thus able to study how meshes adapt to various effects from lack of regularity of solutions and convexity of domains to data smoothness, boundary layers and changing boundary conditions. We note that the implementation of AMFEM is done without enforcing the interior node property in the refinement step.

6.1. Model problem with singularity at the origin. We consider the problem (1.1) in an L -shape domain $\Omega = \{(-1, 1) \times (0, 1)\} \cup \{(-1, 0) \times (-1, 0)\}$ with $\mathbf{w} = r = 0$ and $f = 0$. The exact solution is given by

$$p(\rho, \theta) = \rho^{2/3} \sin(2\theta/3),$$

where ρ, θ are the polar coordinates.

Since this model possesses singularity at the origin, we see in the left figure of Fig 6.1 that the refinement concentrates around the origin, which means the predicted error estimator captures well the singularity of the solution. The right graph of Fig 6.1 reports the estimated and actual errors of the numerical solutions on uniformly and adaptively refined meshes. It can be seen that the error of the stress and displacement in L^2 norm uniformly reduces with a fixed factor on two successive meshes after several steps of iterations, and that the error on the adaptively refined meshes decreases more rapidly than the one on the uniformly refined meshes. This shows that the adaptive mixed finite element method is convergent with respect to the energy error.

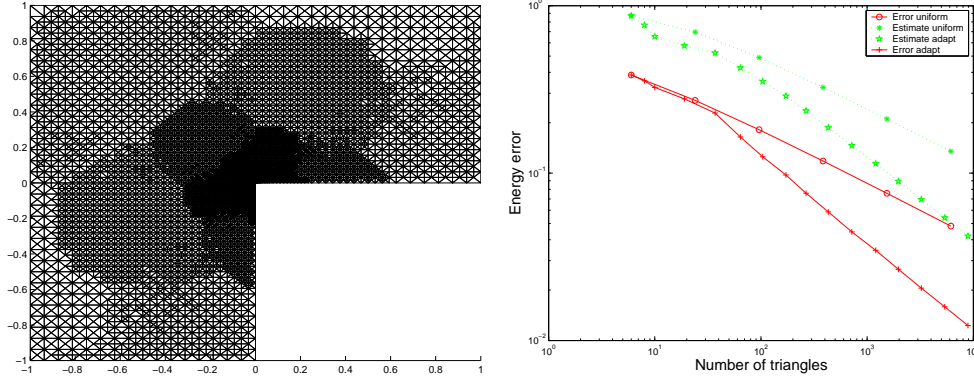


FIG 6.1. A mesh with 14692 triangles (left) and the estimated and actual errors in uniformly / adaptively refined meshes (right) for the marking parameter $\theta = 0.5$.

6.2. Model problem with inhomogeneous diffusion tensor. We consider the problem (1.1) in a square domain $\Omega = (-1, 1) \times (-1, 1)$ with $\mathbf{w} = r = 0$ and $f = 0$, where Ω is divided into four subdomains Ω_i ($i = 1, 2, 3, 4$) corresponding to the axis quadrants (in the counterclockwise direction), and the diffusion-dispersion tensor S is piecewise constant with $S = s_i I$ in Ω_i . This model problem is taken from [24, 36, 39]. We suppose the exact solution of this model has the form

$$p(\rho, \theta) = \rho^\alpha (a_i \sin(\alpha\theta) + b_i \cos(\alpha\theta))$$

in each Ω_i with Dirichlet boundary conditions. Here ρ, θ are the polar coordinates in Ω , a_i and b_i are constants depending on Ω_i , and α is a parameter. We note that The stress solution, $\mathbf{u} = -S\nabla p$, is not continuous across the interfaces, and only its normal component is continuous. It finally exhibits a strong singularity at the origin. We consider two sets of coefficients in the following table:

Case 1	Case 2
$s_1 = s_3 = 5, s_2 = s_4 = 1$	$s_1 = s_3 = 100, s_2 = s_4 = 1$
$\alpha = 0.53544095$	$\alpha = 0.12690207$
$a_1 = 0.44721360, b_1 = 1.00000000$	$a_1 = 0.10000000, b_1 = 1.00000000$
$a_2 = -0.74535599, b_2 = 2.33333333$	$a_2 = -9.60396040, b_2 = 2.96039604$
$a_3 = -0.94411759, b_3 = 0.55555555$	$a_3 = -0.48035487, b_3 = -0.88275659$
$a_4 = -2.40170264, b_4 = -0.48148148$	$a_4 = 7.70156488, b_4 = -6.45646175$

In MARK step, the marking parameter θ , in terms of Dörfler marking, is chosen as 0.7 in the first case and as 0.94 in the second case. Table 6.1 shows for Case 1 some results of the actual error e_k , the a posteriori indicator η_k , the experimental convergence rate, EOC_E , of E_k , and the experimental convergence rate, EOC_η , of η_k , where

$$\text{EOC}_E := \frac{\log(e_{k-1}/e_k)}{\log(\text{DOF}_k/\text{DOF}_{k-1})}, \quad \text{EOC}_\eta := \frac{\log(\eta_{k-1}/\eta_k)}{\log(\text{DOF}_k/\text{DOF}_{k-1})},$$

and DOF_k denotes the number of elements with respect to the k -th iteration. We can see that the convergence rates EOC_E and EOC_η are close to 0.5 as the iteration number $k = 15$, which means the optimal decays of the actual error e_k and the a posteriori error indicator η_k are almost attained after 15 iterations with optimal meshes.

Fig 6.2 shows an adaptively refined mesh with 4763 elements and the estimated and actual errors against the number of elements in adaptively refined meshes for Case 1. Fig 6.3 shows an adaptively refined mesh with 1093 elements and the actual error against the number of elements in adaptively refined meshes for Case 2.

TABLE 6.1

Results of actual error E_k , a posteriori indicator η_k , and their convergence rates EOC_E and EOC_η : Case 1

k	DOF $_k$	e_k	η_k	EOC_E	EOC_η
1	8	1.3665	5.0938	—	—
2	20	1.1346	3.4700	0.2030	0.4189
9	2235	0.1776	1.1115	0.4016	0.4004
11	7165	0.1106	0.7111	0.3851	0.4004
12	13188	0.0871	0.5566	0.3915	0.4015
14	43785	0.0510	0.3365	0.4707	0.4476
15	76770	0.0387	0.2581	0.4915	0.4724

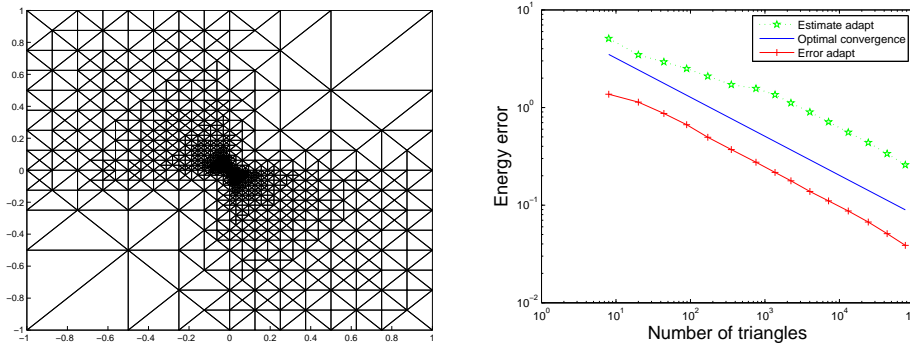


FIG 6.2. A mesh with 4763 triangles (left) and the estimated and actual error against the number of elements in adaptively refined meshes (right): Case 1.

From the left figures of Fig 6.2-6.3, we can see that the refinement concentrates around the origin, which means the AMFEM algorithm detects the region of rapid variation. In the right graphs of Fig 6.2-6.3 each includes an optimal convergence line, which shows in both cases, the energy error performs a trend of descending with an optimal order convergent rate after several steps of adaptive iterations for the problem with strongly discontinuous coefficients. We note that the energy error is approximated with a 7-point quadrature formula in each triangle.

6.3. Convection-dominated model problem: boundary layer. In this example, we take $\Omega = (0, 1) \times (0, 1)$ in \mathbb{R}^2 , and choose $\mathbf{w} = (1, 1)$ and $r = 0$. Further, we set $p = 0$ on $\partial\Omega$, and select the right-hand side f such that the analytical solution to (1.1) is given by

$$p(x, y) = \left(\frac{\exp(\frac{x-1}{\varepsilon}) - 1}{\exp(-\frac{1}{\varepsilon}) - 1} + x - 1 \right) \left(\frac{\exp(\frac{y-1}{\varepsilon}) - 1}{\exp(-\frac{1}{\varepsilon}) - 1} + y - 1 \right).$$

The solution is smooth, but has boundary layers at $x = 1$ and $y = 1$, with layer width of order $\mathcal{O}(\varepsilon)$. This problem is well-suited to test whether the estimator is able to pick up the steep gradients near these boundaries.

We start computations from the origin mesh consisted of 8 right-angled triangles, and we choose the marking parameter $\theta = 0.5$ in the adaptive algorithm AMFEM.

Fig 6.4 shows the mesh with 10838 triangles (left) and the postprocessing approximation to the scalar displacement p on the corresponding adaptively refined mesh (right) in the case

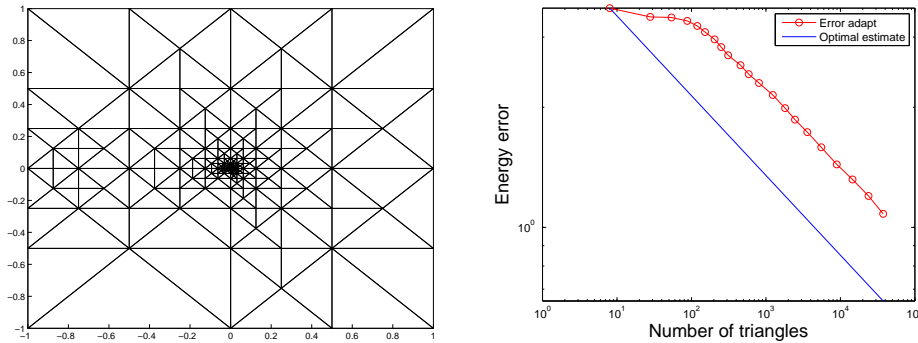


FIG 6.3. A mesh with 1093 triangles (left) and the actual error against the number of elements in adaptively refined mesh (right): Case 2.

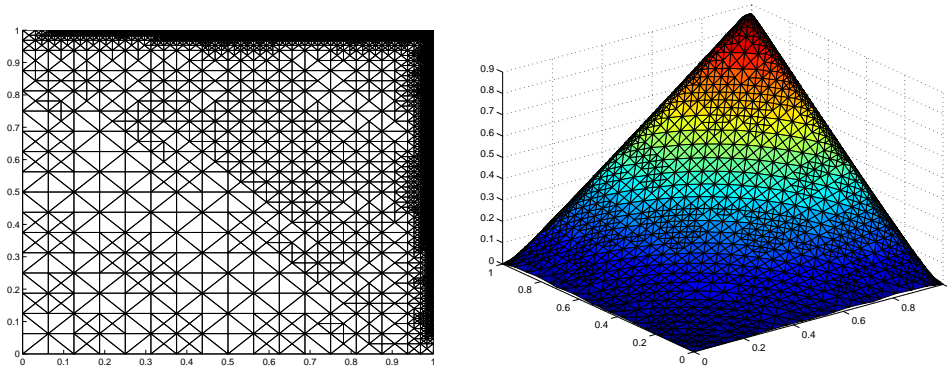


FIG 6.4. A mesh with 10838 triangles (left) and postprocessing approximate displacement on the corresponding adaptively refined mesh (right) for $\varepsilon = 0.01$.

$\varepsilon = 0.01$. Here the value of the postprocessing approximation on each vertex is taken as the arithmetic mean of the values of the displacement finite element solution on all the elements sharing the vertex. The reason for the postprocessing is that the displacement finite element solution is not continuous on each vertex of the triangulation. We see that the refinement focuses around boundary layers, which indicates that the estimators actually capture boundary layers and resolve them in convection-dominated regions. In addition, the postprocessing approximation to the scalar displacement obtains satisfactory results.

Fig 6.5 shows the actual error (energy error) results against the number of elements in adaptively refined meshes for $\varepsilon = 0.1$ (left) and $\varepsilon = 0.01$ (right), including two theoretically-optimal order $(-1/2)$ convergence lines. We see that in each case the actual error descends almost at the optimal rate of convergence after several steps of iterations. The numerical results confirm our theoretical analysis.

6.4. Convection-dominated model problem: interior and boundary layer. Set the domain $\Omega = [-1, 1] \times [-1, 1]$ with non-homogeneous Dirichlet boundary conditions, the velocity field $\mathbf{w} = (2, 1)$, and the reaction term $r = 0$ in (1.1). The source term $f = 0$, the Dirichlet boundary conditions are as follows: $p = 0$ along the left and top sides of the square and $p = 100$ along the right and bottom sides. The exact solution of this problem is unknown,

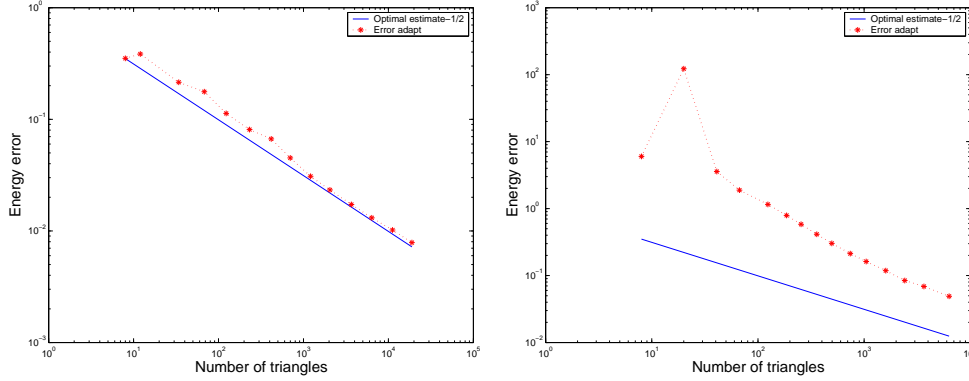


FIG 6.5. Actual error against the number of elements in adaptively refined meshes for $\varepsilon = 0.1$ (left) and $\varepsilon = 0.01$ (right) for the marking parameter $\theta = 0.5$.

but it is known that it exhibits an exponential boundary layer at the boundary $x = 1, y > 0$ and a parabolic interior layer along the line connecting the points $(-1, -1)$ and $(1, 0)$.

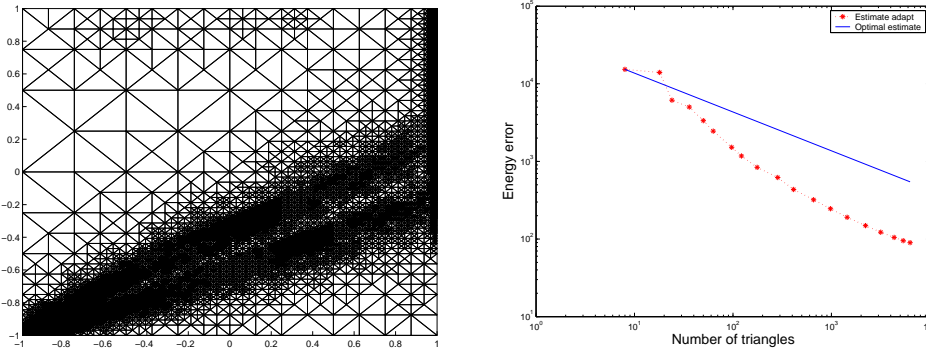


FIG 6.6. A mesh with 47324 elements (left) for $\varepsilon = 0.01, \theta = 0.8$ and estimated error against the number of elements in adaptively refined meshes (right) for $\varepsilon = 0.1, \theta = 0.5$.

We still perform the AMFEM algorithm described in section 2 from the origin mesh consisted of 8 right-angled triangles. From the left graph of Fig 6.6, we can see that when using adaptive refinement the mesh concentrates close to the exponential and parabolic layers. We note that the refinement first occurs close to the region $x = 1, y > 0$, since the exponential layer is more stronger than the parabolic layer. The left graph also illustrates that the a posteriori error estimator exactly capture the behavior of the solution. The right graph of Fig 6.6 shows that the estimated error rapidly reduces starting from the fourth step of iterations, and reaches the optimal rate $(-1/2)$ of convergence until the seventeenth step. This convergence result is consistent with our theoretical analysis.

REFERENCES

- [1] M. Anisworth and J.T.Oden, A posteriori error estimation in finite element analysis, Wiley, Chichester, 2000.
- [2] D.N. Arnold, R.S.Falk and R.Winther. Finite element exterior calculus, homological techniques, and applications. Acta Numerica, pages 1-155, 2006.
- [3] I. Babuska and W. Rheinboldt, A posteriori error estimates for the finite element method, Internat. J. Numer. Methods Engrg, 1978, 12, 1597-1615.

- [4] I. Babuska and W. Rheinboldt, Error estimates for adaptive finite element computations, *SIAM J. Numer. Anal.*, 1978, 15, 736-754.
- [5] I. Babuska and T. Strouboulis, *The finite element method and its reliability*, Clarendon Press, Oxford, 2001.
- [6] R. Becker, S. Mao, An optimally convergent adaptive mixed finite element method, *Numer. Math.*, 2008, 111: 35-54.
- [7] F. Brezzi and M. Fortin, *Mixed and hybrid finite element methods*, Springer, Berlin-Heidelberg-New York, 1991.
- [8] J.M. Cascon, C. Kreuzer, R.H. Nochetto and K.G. Siebert, Quasi-optimal convergence rate for an adaptive finite element method, *SIAM J. Numer. Anal.*, 2008, 46(5): 2524-2550.
- [9] C. Carstensen, A posteriori error estimate for the mixed finite method, *Math. Comp.*, 66(218), 1997, 465-476.
- [10] C. Carstensen and R.H.W. Hoppe, Error reduction and convergence for an adaptive mixed finite element method, *Math. Comp.*, 2006, 75, 1033-1042.
- [11] C. Carstensen and J. Hu, A unifying theory of a posteriori error control for nonconforming finite element methods, *Numer. Math.*, 2007, 107, 473-502.
- [12] C. Carstensen, J. Hu, A. Orlando, Framework for the a posteriori error analysis of nonconforming finite elements, *SIAM J. Numer. Anal.*, 2007, 45, 6882.
- [13] C. Carstensen and H. Rabus, An optimal adaptive mixed finite element method, *Math. Comp.*, 80 (2011), 649667.
- [14] L. Chen, M. Holst and J.C. Xu, Convergence and optimality of adaptive mixed finite element methods, *Math. Comp.*, 2009, 78(265) :35-53.
- [15] P. G. Ciarlet, *The finite element method for elliptic problems*. Nort-Holland, Amsterdam, 1978.
- [16] A. Demlow and R. Stevenson, Convergence and quasi-optimality of an adaptive finite element method for controlling L^2 errors, *Math. Comp.*, 2011, 117 :185-218.
- [17] J. R. Douglas and J. E. Roberts, Global estimates for mixed methods for second elliptic equations, *Math. Comp.*, 44 (1985), 39-52.
- [18] S.H. Du and X.P. Xie, Residual-based a posteriori error estimates of nonconforming finite element method for elliptic problem with Dirac delta source terms, *Science in China Series A: Mathematics*, 2008, 51(8): 1440-1460.
- [19] S.H. Du and X.P. Xie, Error reduction, convergence and optimality of an adaptive mixed finite element method, *Journal of systems science and complexity*, 2011, 24: 1-14.
- [20] S.H. Du and X.P. Xie, Error reduction, convergence and optimality for adaptive mixed finite element methods for diffusion equations, *Journal of Computation Mathematics*, 2012, 30 (5): 483-503.
- [21] S.H. Du and X.P. Xie, A new residual-based posteriori error estimators for lowest-order Raviart-Thomas element approximation to convection-diffusion-reaction equations, *J. Comput. Math.*, revision resubmitted
- [22] S.H. Du, A new residual posteriori error estimates of mixed finite element methods for convection-diffusion-reaction equations, *Numerical methods of PDE*, accepted.
- [23] W. Dörfler, A convergent adaptive algorithm for Poisson's equation, *SIAM J. Numer. Anal.*, 1996, 33, 1106-1124.
- [24] G. T. Eigestad and R. A. Klausen, On the convergence of the multi-point flux O -method: Numerical experiments for discontinuous permeability, *Numer. Methods Partial Differential Equations*, 21 (2005), 1079-1098.
- [25] R. Hiptmair, Canonical construction of finite elements. *Mathematics of Computation*, 1999, 68: 1325-1346.
- [26] J. Hu, Z.C. Shi and J.C. Xu, Convergence and optimality of the adaptive finite element method. *Research Report*, 19(2009), School of Mathematical Science and Institute of Mathematics, Peking University, available at www.math.pku.edu.cn:800/var/preprint/7197.pdf; *Numer. Math.*, to appear.
- [27] K. Mekchay and R.H. Nochetto, Convergence of adaptive finite element methods for general second linear elliptic PDEs, *SIAM J. Numer. Anal.*, 2005, 43: 1803-1827.
- [28] W.F. Mitchell, A comparison of adaptive refinement techniques for elliptic problems. *ACM Trans. Math. Soft.*, 1989, 15(4): 326-347.
- [29] W.F. Mitchell, Optimal multilevel iterative methods for adaptive grids. *SIAM Journal on Scientific and Statistical Computing*, 1992, 13: 146-167.
- [30] P. Morin, R.H. Nochetto and K.G. Siebert, Data oscillation and convergence of adaptive FEM, *SIAM J. Numer. Anal.*, 2000, 38(2): 466-488.
- [31] P. Morin, R.H. Nochetto and K.G. Siebert, Local problems on stars: a posteriori error estimators, convergence, and performance, *Math. Comp.*, 2003, 72 (243): 1067-1097.
- [32] P. Morin, R.H. Nochetto and K.G. Siebert, Convergence of adaptive finite element methods, *SIAM Review*, 2002, 44(4), 631-658.
- [33] M.C. Rivara, Mesh refinement processes based on the generalized bisection of simplices. *SIAM J. Numer. Anal.*, 1984, 21: 604-613.
- [34] M.C. Rivara, Design and data structure for fully adaptive, multigrid finite element software. *ACM Trans. Math. Soft.*, 1984, 10 :242-264
- [35] P. A. Raviart and J. M. Thomas, A mixed finite element method for 2nd order elliptic problems, in *Mathe-*

- mathematical Aspects of Finite Element Methods (Proceedings of the Conference of the C.N.R., Rome, 1975), Lecture Notes in Math. 606, Springer, Berlin, 1977, 292-315.
- [36] B. Riviere and M. F. Wheeler, A posteriori error estimates for a discontinuous Galerkin method applied to elliptic problems, *Comput. Math. Appl.*, 46 (2003), 141C163.
 - [37] E.G. Sewell, Automatic generation of triangulations for piecewise polynomial approximation. In Ph. D. dissertation. Purdue Univ., West Lafayette, Ind., 1972.
 - [38] R. Verfürth, A review of a posteriori error estimation and adaptive mesh-refinement techniques, Wiley-Teubner, 1996.
 - [39] M. Vohralík, A posteriori error estimates for lowest-order mixed finite element discretizations of convection-diffusion-reaction equations, *SIAM J. Numer. Anal.*, 45(4), 2007, 1570-1599.